Open Access

Influence of Water Molecules on Properties of Binuclear or Bridged Structures for Chiral Cu^{II}-Ni^{II}, Cu^{II}-Pd^{II}, and Cu^{II}-Pt^{II} Tetracyano-Bimetallic Assemblies

Takashiro Akitsu* Yuki Endo, Minoru Okawara, Yusuke Kimoto and Mao Ohwa

Department of Chemistry, Faculty of Science, Tokyo University of Science, 1-3 Kagurazaka, Shinjuku-ku, Tokyo 162-8601, Japan

Abstract: We have prepared new chiral bimetallic assemblies of discrete binuclear $[CuL_2][Ni(CN)_4]\cdot 2H_2O$ or one-dimensional cyanide-bridged $[CuL_2][Pd(CN)_4]$ (and $[CuL_2][Pt(CN)_4]$) (L = (*1S,2S*)-(+)-*N,N'*-dimethyl-cyclohexane-1,2-diamine). The numbers of co-crystallized water molecules contained are different from each other and their compositions are easy to vary due to co-crystallized water molecules. As far as we studied on the related $[Cu(diamine)_2]_a[M(CN)_b]_c\cdot dH_2O$ compounds, actually such a feature has been found for the first time. According to crystal structures, the elongated axial bond distances of $[CuL_2]^{2+}$ moieties are Cu-N = 2.195(7) Å for $[CuL_2][Ni(CN)_4]\cdot 2H_2O$, Cu-N = 2.443(4) and 2.519(2) Å for $[CuL_2][Pd(CN)_4]$. Single crystal structure analyses, variable low temperature XRD, measurements of electronic, CD, emission, and XPS spectra and magnetic properties have been carried out. We compared their structural preference between Ni^{II} and Pd^{II} (or Pt^{II}) metal ions. Novel emission band of $[CuL_2][Pt(CN)_4]$ appeared at 410 nm (λ_{ex} = 360 nm) in the solid state regardless of quenching by cyanide-bridged $[CuL_2]^{2+}$ moieties.

Keywords: Copper(II), Nickel(II), Palladium(II), Platinum(II), Cyanide.

INTRODUCTION

In recent years, cyanide-bridged coordination polymers [1, 2] and their various functions and multifunctions such as photomagnets [3-7] and chiral magnets [8-14], including *N,N'*-dimethyl-cyclohexane-1,2-diamine ligands [14], have been studied vigorously. From the viewpoint of crystal engineering, structural dimensionality, flexibility (static structural strain and dynamic structural changes by external physical stimulus), and tuning of electronic properties by these factors are important things for rational design of functional materials. In this context, even slight strain of crystal lattices may play a significant role in obvious switching of electronic properties [15, 16]. Indeed, negative thermal expansion of cyanide-bridged coordination polymers is caused by not only lattice strain by appropriate vibrational modes of cyanides but also reversible inclusion or release of co-crystallized water molecules [17, 18].

Structural tuning caused by co-crystallized water molecules is also known for some cyanide-bridged systems. For example, a chiral coordination polymer, $[Cu(RR\text{-chxn})_2][Ni(CN)_4]\cdot nH_2O$ (*RR*-chxn = *trans*-cyclohexane-(*1R,2R*)-diamine), loses co-crystallized water molecules on heating accompanying with structural change from one-dimensional zigzag structure (n = 2) to one-dimensional straight one (n = 0) [19]. Originally, we reported on novel axial coordination bonds of pseudo Jahn-Teller elongation and semi-coordination indicating ionic character for $[Cu(RR\text{-chxn})_2][M(CN)_4]\cdot 2H_2O$ complexes [20, 21]. The long axial interatomic distances are Cu-N = 3.120(8) Å, 3.092(8) Å, and 3.09(1) Å for M = Ni [20], Pd [21], and Pt [20], respectively. Moreover, we have systematically studied on cyanide-bridged bimetallic assemblies containing Cu^{II} ions of mononuclear [22-26], straight one-dimensional [27, 28], two-dimensional ones [29, 30], and co-crystals of mononuclear and one-dimensional ones [30]. Dimensionality, steric factors, and ionic radii, in particular the magnitude of Jahn-Teller distortion of Cu^{II} moiety, may be important factors for crystal packing.

Herein we report on new chiral bimetallic assemblies of discrete binuclear $[CuL_2][Ni(CN)_4]\cdot 2H_2O$ or one-dimensional cyanide-bridged $[CuL_2][Pd(CN)_4]$ (and $[CuL_2][Pt(CN)_4]$) (L = (*1S,2S*)-(+)-*N,N'*-dimethyl-cyclohexane-1,2-diamine) tuned by variable number of co-crystallized water molecules. The diamine ligand L is similar to *RR*-chxn but it has bulky methyl groups in coordinating atoms. As far as we studied on $[Cu(diamine)_2]_a[M(CN)_b]_c\cdot dH_2O$ complexes, such structural features was observed for the first time. In this study, "tuning" means being one of the dominating factors for regulating structures (and changing structures) in the crystals. Preparations, crystal structures, variable low temperature XRD, electronic, CD, emission, and XPS spectra and magnetic properties have been examined for comparison of Ni^{II}, Pd^{II}, and Pt^{II} metal ions.

MATERIALS AND METHODOLOGY

General Procedure

The precursor complex, $[CuL_2(H_2O)_2](NO_3)_2$, was prepared according to the literature procedure by using the corresponding ligands [31]. Commercially available (*1S,2S*)-(+)-*N,N'*-dimethyl-cyclohexane-1,2-diamine (TCI) and the

---

*Address correspondence to this author at the Department of Chemistry, Faculty of Science, Tokyo University of Science, 1-3 Kagurazaka, Shinjuku-ku, Tokyo 162-8601, Japan; Tel: +81-3-5228-8271; Fax; +81-3-5261-4631; E-mail: akitsu@rs.kagu.tus.ac.jp

rest of reagents and solvents (Aldrich) were used as received without further purification.

Preparation of $[CuL_2][Ni(CN)_4]\cdot 3H_2O$ (1)

Slow diffusion of aqueous solution (10 mL) of $[CuL_2(H_2O)_2](NO_3)_2$ precursor (0.397 g, 0.78 mmol) onto aqueous solution (10 mL) of $K_2[Ni(CN)_4]$ (0.188 g, 0.78 mmol) gave rise to blue microcrystals at 298 K immediately. Single crystals suitable for X-ray analysis were also grown in the same solutions for a few days. Yield 62.2 %. Anal. Calcd for $C_{20}H_{42}CuN_8NiO_3$: C, 42.53; H, 7.49; N, 19.84. Found: C, 42.84; H, 7.67; N, 19.81. TG-DTA: weight loss 9.61 % ($3H_2O$) up to 492 K (decomposition). IR (Nujol, cm^{-1}): 417, 665, 721, 887, 947, 1008, 1066, 1160, 1377, 1461, 2125, 2148 (cyanide), 2854, 2927, 3200, 3434. XRF: 8.049 keV (CuKα), 7.479 keV (NiKα).

Preparation of $[CuL_2][Pd(CN)_4]\cdot H_2O$ (2)

Slow diffusion of aqueous solution (10 mL) of $[CuL_2(H_2O)_2](NO_3)_2$ precursor (0.118 g, 0.23 mmol) onto aqueous solution (10 mL) of $K_2[Pd(CN)_4]$ (0.066 g, 0.23 mmol) gave rise to blue microcrystals at 298 K immediately. Single crystals suitable for X-ray analysis were also grown in the same solutions for a few days. Yield 87.9 %. Anal. Calcd for $C_{20}H_{38}CuN_8OPd$: C, 41.67; H, 6.64; N, 19.44. Found: C, 41.36; H, 6.55; N, 19.20. TG-DTA: weight loss 3.15 % (H_2O) up to 474 K (decomposition). IR (Nujol, cm^{-1}): 450, 665, 721, 935, 1161, 1302, 1376, 1462, 2125, 2136 (cyanide), 2170, 2670, 2727, 2855, 2925, 3201, 3398, 3582. XRF: 8.049 keV (CuKα).

Preparation of $[CuL_2][Pt(CN)_4]\cdot 1.5H_2O$ (3)

Slow diffusion of aqueous solution (10 mL) of $[CuL_2(H_2O)_2](NO_3)_2$ precursor (0.116 g, 0.23 mmol) onto aqueous solution (10 mL) of $K_2[Pt(CN)_4]$ (0.099 g, 0.23 mmol) gave rise to blue microcrystals at 298 K immediately. Yield 95.0 %. Anal. Calcd for $C_{20}H_{39}CuN_8O_{1.5}Pt$: C, 35.63; H, 5.83; N, 16.62. Found: C, 35.63; H, 5.81; N, 16.61. TG-DTA: weight loss 4.01 % ($1.5H_2O$) up to 486 K (decomposition). IR (Nujol, cm^{-1}): 480, 665, 721, 934, 1158, 1302, 1376, 1462, 2126, 2136 (cyanide), 2174, 2361, 2726, 2854, 2923, 3185, 3434, 3582. XRF: 8.049 keV (CuKα).

Physical Measurements

Elemental analyses (C, H, N) were carried out on a Perkin Elmer 2400II CHNS/O analyzer at Tokyo University of Science. Infrared spectra were recorded as Nujol mull on a JASCO FT-IR 460 plus spectrophotometer in the range of 4000-400 cm^{-1} at 298 K. Diffuse reflectance electronic spectra were measured on a JASCO V-560 spectrophotometer equipped with an integrating sphere in the range of 1000-220 nm at 298 K. Circular dichroism (CD) spectra were measured as KBr pellets on a JASCO J-820 spectropolarimeter in the range of 800-200 nm at 298 K. Luminescence excitation and emission spectra of the solid compounds were recorded by a JASCO FP-6200 spectrofluorometer using a sample holder developed for powders at 298 K. Powder XRD patterns were recorded with a Rigaku Rint 2000 diffractometer employing Cu Kα radiation (λ = 1.54184 Å). Powder XRD patterns were also measured by using synchrotron radiation beamline at KEK-PF BL-8B with 8 keV (λ = 1.54184 Å) under variable temperature apparatus of nitrogen stream equipped with a Rigaku imaging plate. All the samples were measured for 3 min and constant ring current (440 mA). The magnetic properties were investigated with a Quantum Design MPMS-XL superconducting quantum interference device magnetometer (SQUID) at an applied field 5000 Oe in a temperature range 5-300 K. Powder samples of 39.31, 40.47, and 40.31 mg for **1**, **2**, and **3**, respectively, were measured in a pharmaceutical cellulose capsule. The apparatus signals and the diamagnetic corrections were evaluated from Pascal's constants. The temperature-independent paramagnetism was not added to the data set. X-ray photoelectron spectra (XPS) were recorded with a JEOL JPS-9010MC at 298 K. Powder samples were pressed as pellets and put under ultra high vaccum to reach the 10^{-8} Pa range. The nonmonochromatized Mg Kα source was used at 10 kV and 10 mA, as a flood gun to compensate for the nonconductive samples. The binding energy of the spectra was calibrated in relation to the C 1s binging energy, which was applied as an internal standard. X-ray fluorescence spectra (XRF) were measured with a PANalytical Epsilon 5 by using Ge Kα source at 298 K. The thermal gravimetry (TG) and the differential thermal analysis (DTA) were recorded on a Rigaku TG8120 instruments in the atomosphere at a heating rate of 10 K/min. α-alumina was used as the reference sample, and the examined samples of **1**, **2**, and **3** were 4.438, 4.157, and 3.597 mg, respectively.

X-ray Crystallography

Blue prismatic single crystals of **1** (0.161 x 0.112 x 0.106 mm) and blue violet prismatic single crystals of **2** (0.180 x 0.080 x 0.040 mm) were glued on top of a glass fiber and coated with a thin layer of epoxy resin to measure the diffraction data. The X-ray intensities were measured at 100 K for **1** with graphite-monochromated Mo Kα radiation (λ = 0.71073 Å) on a Bruker APEX2 CCD diffractometer. The structures were solved by direct methods using SHELXS97 [32] and expanded by Fourier techniques in a SAINT program package [33] (including SHELXTL version). The structures were refined on F^2 anisotropically for non-hydrogen atoms by full-matrix least-square methods with SHELXL97 [32]. Empirical absorption corrections were applied by a program SADABS [34]. The hydrogen atoms were included in geometrically calculated position with C-H = 0.980 Å and refined by using riding model. Since hydrogen atoms could not be observed in the difference Fourier map, we could not introduce hydrogen atoms of water molecules connected to O1 and O2 atoms for **1**. Although residual electron density was also found in the difference Fourier maps, the models containing these peaks as water molecules resulted in increase of R-values. Therefore, we could not assign them and we could not discuss hydrogen bonds closely. These bad results in refinement are mainly due to thermal vibration of oxygen atoms of co-crystallized water. Although we have tried some cases of model structures, we can not set suitable restraint or constraint without bias or unreasonable results. Therefore, we employed the present result as described. Unfortunately, single crystals suitable for X-ray analysis could not be obtained for **3**.

Crystallographic data for **1**. $C_{20}H_{36}CuN_8NiO_2$, triclinic, *P1*, a = 9.071(4) Å, b = 9.371(4) Å, c = 8.842(4) Å, α = 80.077(5)°, β = 69.545(5)°, γ = 72.407(5)°, and V = 669.4(5) Å^3, and Z = 1, M = 100(2) K, D_c = 1.401 Mgm^{-3}, R_1 = 0.0486,

wR_2 = 0.1326 (3788 reflections), S = 1.000, T = 100(2) K, μ = 1.533 mm^{-1}. Flack value is equal to -0.09(2).

Crystallographic data for **2**. $C_{20}H_{36}CuN_8Pd$, orthorhombic, $P2_12_12_1$, a = 10.393(4) Å, b = 12.565(5) Å, c = 18.527(7) Å, and V = 2419.4(17) Å^3, and Z = 4, M = 558.51, D_c = 1.533 Mgm^{-3}, R_1 = 0.0424, wR_2 = 0.1151 (5439 reflections), S = 0.817, T = 173(2) K, μ = 1.645 mm^{-1}. Flack value is equal to -0.01(5).

RESULTS AND DISCUSSION

Molecular structure of **1** is depicted in Fig. (**1**) and selected bond distances and angles of **1** are described in the caption. Complex **1** is consisted of a discrete binuclear Cu^{II}-Ni^{II} complex linked by one cyanide-bridge and two molecules of co-crystallized water. The Cu^{II} ion affords a distorted five-coordinated square pyramidal [CuN_5] coordination geometry with Cu-N = 2.195(7) Å. A conventional index of the degree of Jahn-Teller distortion, T, is defined by the ratio of equatorial Cu-N bond distances / axial Cu-N bond distances [35]. The magnitude of distortion of axial bonds can be described to be T = 0.935 for **1**. The [$Ni(CN)_4$]$^{2-}$ moiety affords a square planar coordination geometry being in accordance with other examples associated with Ni^{II} bond radii [36] and cyanide groups. In contrast to short axial bond of Cu-N-C = 138.3(6)° and novel long axial semi-coordination bond of Cu-N-C = 97.5(1)° in [Cu(*RR*-chxn)$_2$][M(CN)$_4$]·2H$_2$O [20], the present bond angles of Cu1-N1-C1 = 157.5(6)° between linked two chromophores of **1** are found as a normal axial coordination bond of Jahn-Teller distortion. Obvious hydrogen bonds are formed by cyanide H-acceptors for **1**. The *trans* cyanide (N3) H-acceptor connected to an amino hydrogen atom, while the *cis* cyanide (N2 and N4) H-acceptor connected to two water hydrogen atoms.

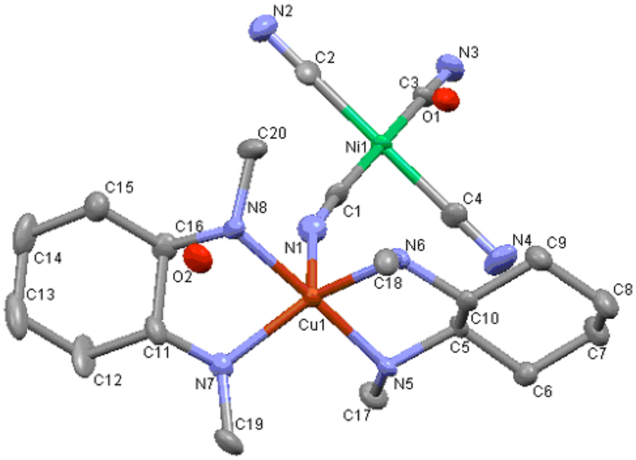

Fig. (1). Molecular structure of **1** showing the atom labeling scheme. Displacement ellipsoids are drawn at the 30 % probability level. Hydrogen atoms are omitted for clarity. Selected bond distances (Å) and angles (°): Cu1-N1 = 2.195(7), Cu1-N5 = 2.017(6), Cu1-N6 = 2.049(5), Cu1-N7 = 2.090(6), Cu1-N8 2.056(5), Ni1-C1 = 1.872(6), Ni1-C2 = 1.870(7), Ni1-C3 = 1.846(7), Ni1-C4 = 1.845(7), C1-N1 = 1.153(9), C2-N2 = 1.146(10), C3-N3 = 1.166(9), C4-N4 = 1.168(10), N5-Cu1-N8 = 178.2(2), N6-Cu1-N7 = 153.1(2), N1-Cu1-N6 = 104.3(2), N1-Cu1-N7 = 102.6(2), N5-Cu1-N6 = 85.0(2), N6-Cu1-N8 = 95.8(2), N5-Cu1-N7 = 95.0(2), N7-Cu1-N8 = 83.6(2), N1-Cu1-N5 = 91.7(2), N1-Cu1-N8 = 89.6(2), C1-Ni1-C3 = 178.6(3), C2-Ni1-C4 = 179.3(4), N1-C1-Ni1 = 176.0(6), Cu1-N1-C1 = 157.5(6).

Molecular structure of **2** is depicted in Fig. (**2**) and selected bond distances and angles of **2** are described in the caption. Complex **2** is consist of cyanide-bridged bimetallic assemblies showing alternating arrangement of [CuL_2]$^{2+}$ and [$Pd(CN)_4$]$^{2-}$ moieties without co-crystallized water molecules. The Cu^{II} ion affords a six-coordinated distorted octahedral [CuN_6] coordination geometry exhibiting Jahn-Teller distortion of Cu-N = 2.443(4) and 2.519(2) Å. The degree of distortion of axial bonds can be represented as T = 0.840 and 0.814, respectively. The [$Pd(CN)_4$]$^{2-}$ moiety affords a square planar coordination geometry being in accordance with other compounds. Even short side of axial bonds, the bond angle of Cu1-N1-C1 = 141.2(4)° suggests that the [CuL_2]$^{2+}$ and [$Pd(CN)_4$]$^{2-}$ chromophores are strongly interacted *via* bent bridges having slightly overlapped orbitals. Along the one-dimensional cyanide-bridges of **2**, hydrogen bonds are formed *via* bridging cyanide (N3) H-acceptor connected to an amino hydrogen atom. While free cyanide (N4) H-acceptor connected to another amino hydrogen atom.

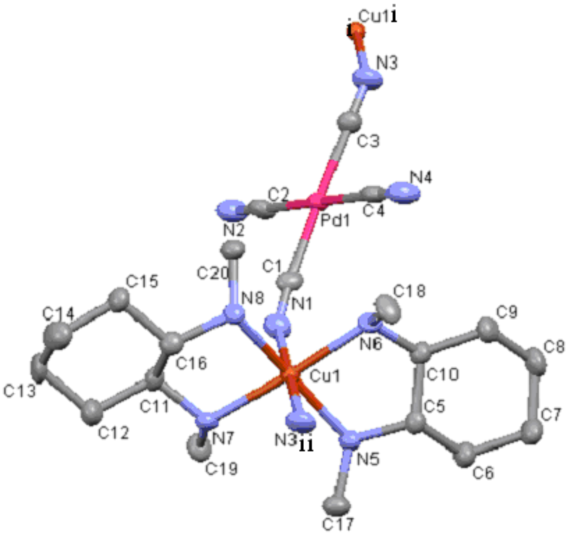

Fig. (2). Molecular structure of **2** showing the atom labeling scheme. Displacement ellipsoids are drawn at the 30 % probability level. Hydrogen atoms are omitted for clarity. [Symmetry codes: (i) x+1, y, z; (ii) x-1, y, z]. Selected bond distances (Å) and angles (°): Cu1-N1 = 2.443(4), Cu1-N3^{ii} = 2.519(2), Cu1-N5 = 2.048(4), Cu1-N6 = 2.048(4), Cu1-N7 = 2.066(4), Cu1-N8 = 2.042(3), Pd1-C1 = 1.986(5), Pd1-C2 = 2.005(5), Pd1-C3 = 1.991(5), Pd1-C4 = 1.984(5), C1-N1 = 1.158(6), C2-N2 = 1.134(6), C3-N3 = 1.144(7), C4-N4 = 1.148(6), N5-Cu1-N8 = 171.88(18), N6-Cu1-N7 = 174.19(16), N6-Cu1-N8 = 93.98(15), N5-Cu1-N6 = 84,77(16), N7-Cu1-N8 = 85,21(16), N5-Cu1-N7 = 96.83(16), N1-Cu1-N8 = 96.50(17), N1-Cu1-N6 = 87.72(16), N1-Cu1-N5 = 91.47(15), N1-Cu1-N7 = 86.66(15), C1-Pd1-C3 = 179.8(2), C2-Pd1-C4 = 179.8(2), N1-C1-Pd1 = 172.6(4),Cu1-N1-C1 = 141.2(4).

As recent studies of heating indicated [19], some cyanide-bridged coordination polymers exhibit reversible structural changes accompanying with losing or containing co-crystallized water molecules. Because of bulky organic ligands and steric factors due to ionic radii of M^{2+} ions in [$M(CN)_4$]$^{2-}$ moieties, complexes **1**-**3** take predominant (bridged or discrete) structures as determined. Because powder samples are easy to lose co-crystallized water molecules even at room temperature, their compositions, powder diffraction, spectral and magnetic data are not reliable in usual sense in view of measurements for stable compositions except for crystal structures based on single crystals. The determined structures of **1** and **2** can be regarded as two opposite sides of variable structures, and actual structures or composites of **1**-**3** may be intermediate of them. They can convert each other continuously by losing co-crystallized water molecules from cyanide-bridged frameworks.

Under such proposition based on experimental facts, powder XRD patterns of **1**-**3** measured with a laboratory system are shown in Fig. **S1**. Three predominant peaks appeared at $2\theta = 10.48$, 13.24, and 16.30° for **1**, $2\theta = 9.42$, 13.94, and 16.90° for **2**, and $2\theta = 9.40$, 13.92, and 16.86° for **3**. The fact that **2** and **3** are similar to each other and different from **1** suggests that **2** and **3** are isostructural, though crystal structure of **3** has not determined yet.

On the other hand, in order to examine thermally-accessible structural changes such as negative thermal distortion [37] and crossover of magnetic orbitals by Jahn-Teller distortion [38, 39], we measured variable temperature (cooling) XRD patterns (Figs. **S2** and **S3**) for structurally-characterized complexes **1** and **2**. The X-ray beam generated from synchrotron radiation with $\lambda = 1.54184$ Å was employed to avoid bad effects of absorption. For cyanide-bridged coordination polymers, heating is important for structural changes associated with co-crystallized water molecules, while cooling is effective for structural distortion resulting from lattice strains. As listed in Table **S1**, parameters derived from Bragg's law ($2d\sin\theta = n\lambda$) indicated that at 100-300 K complexes **1** and **2** exhibited positive (normal) thermal expansion as a function of temperature continuously without structural phase transition nor losing co-crystallized water molecules.

The IR spectra (not shown) of **1** showed strong cyanide stretching peaks at 2125 and 2148 cm^{-1}. The splitting of bands is attributed to the fact that the cyanide ligands coordinates to Cu^{II} ions and three free cyanide ligands. On the other hand, **2** and **3** exhibited the corresponding peaks at 2125 and 2136 cm^{-1} and 2126 and 2136 cm^{-1}, respectively. As for the latter cases, two types (two bridged and two free) of cyanide ligands and weight of metal ions should affect on the results [40].

Diffuse reflectance spectra (Fig. **S4**) showed a broad d-d peak at 16560 cm^{-1} for **1**, 16610 cm^{-1} for **2**, and 16580 cm^{-1} for **3**. Slight increasing of band width of **1** may be attributed to a square pyramidal $[CuN_5]$ chromophore, which is different from elongated octahedral $[CuN_6]$ chromophore of **2** and **3**. The d-d bands are attributed to allowed ${}^2B_{1g}$ -> ${}^2A_{1g}$ and ${}^2B_{1g}$ -> ${}^2E_g$ transitions in D_{4h} symmetry [41]. The $3d_{z2}$ orbital level depends on the axial ligands or distortion of chromophores [42, 43].

The corresponding CD spectra in KBr pellets (Fig. **S4**) exhibited a broad d-d peak at 17100 cm^{-1} for **1**, 17200 cm^{-1} for **2**, and 17200 cm^{-1} for **3**. Similarly to the diffuse reflectance spectra, spectral feature of **1** is slightly different from that of **2** and **3**, namely shift of low-wavenumber tail of charge transfer bands at 21700, 21700, and 21800 cm^{-1} for **1**, **2**, and **3**, respectively.

Although quenching by $[CuL_2]^{2+}$ moieties was expected, **3** exhibited novel emission band at 410 nm ($\lambda_{ex} = 360$ nm) from $[Pt(CN)_4]^{2-}$ moiety in the solid states (Fig. **3**). Indeed, $[Cu(RR\text{-chxn})_2][Pt(CN)_4]\cdot 2H_2O$ did not exhibit such emission [20]. The present example is the second example among the related compounds.

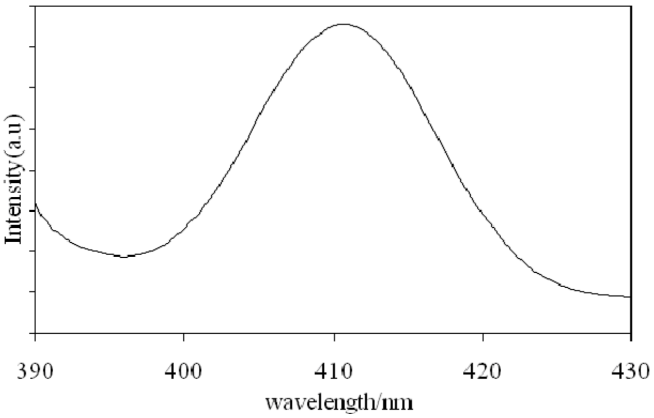

Fig. (3). Solid state emission spectra ($\lambda_{ex} = 360$ nm) for **3** at 298 K.

The XPS of **1**-**3** were measured in the range 0 - 1000 eV at 298 K. The peaks of C 1s, N 1s, and O 1s appeared at 284, 399, and 531 eV, respectively. As for organic ligand moieties, these features are similar to the related complexes [20, 21, 27]. The Cu $2p_{1/2}$ and Cu $2p_{3/2}$ peaks appeared at 954 and 934 eV, respectively for **1**-**3** (Fig. **S5**). These signals do not show abnormal peak separation nor the satellite structure typical of Cu^{I} derivatives, which confirms the Cu^{II} valence state. As for $[M(CN)_4]^{2-}$ moieties, the Ni $2p_{3/2}$ and Ni $2p_{1/2}$ peaks appeared at 874 and 856 eV for **1** (Fig. **S6**), the Pd $3d_{5/2}$ and Pd $3d_{3/2}$ peaks appeared at 345 and 340 eV for **2** (Fig. **S7**), and the Pt $4f_{5/2}$ and Pt $4f_{7/2}$ peaks appeared at 78 and 74 eV for **3** (Fig. **S8**). Coordination number is an important factor for shifting XPS peaks [27].

The magnetic moments (Fig. **S9**) exhibited considerably smaller values in the higher temperature region than expected values for magnetically diluted Cu^{II} compounds with $s = 1/2$, though the related one-dimensional complexes exhibited weak antiferromagneic interactions *via* cyanide-bridges [44-47]. However, we have also observed similar cases that cyanide-bridged bimetallic assemblies of Cu^{II} ($s=1/2$) and Ni^{II}, Pd^{II}, and Pt^{II} ($s = 0$) exhibit small magnetization at high temperature region. These compounds are not straight one-dimensional bridges but zigzag bridges. Therefore, weak superexchange antiferromagnetic interaction without sufficiently overlapped orbitals results in diamagnetic behavior by $[M^{II}(CN)_4]^{2-}$ moieties.

CONCLUSION

We have reported three chiral bimetallic assemblies of discrete binuclear $[CuL_2][Ni(CN)_4]\cdot 2H_2O$ (**1**) or one-dimensional cyanide-bridged $[CuL_2][Pd(CN)_4]$ (**2**) and $[CuL_2][Pt(CN)_4]$ (**3**) tuned by the numbers of co-crystallized water molecules. As far as we have studied on the related compounds systematically, compounds having easily variable compositions (and structures) of co-crystallized water molecules have been found for the first time. Novel emission band of $[Pt(CN)_4]^{2-}$ moiety appeared for **3** also supports relatively weak interaction between $[CuL_2]^{2+}$ and $[M(CN)_4]^{2-}$ moieties in the bridged structure.

SUPPLEMENTARY DATA

Supplementary material is available on the publishers web site along with the published article.

ACKNOWLEDGEMENTS

We are gratefully acknowledged to Institute for Molecular Science for measurement of magnetism and KEK-PF BL-8B (2008G526) for X-ray crystallography using synchrotron radiation.

REFERENCES

[1] Ohba M, Okawa H. Synthesis and magnetism of multi-dimensional cyanide-bridged bimetallic assemblies. Coord Chem Rev 2000; 198: 313-28.

[2] Okawa H, Ohba M. Structures and magnetism of cyanide-bridged bimetallic compounds: design of complex-based magnetic materials. Bull Chem Soc Jpn 2002; 75: 1191-203.

[3] Sato O. Optically switchable molecular solids: photoinduced spin-crossover, photochromism, and photoinduced magnetization. Acc Chem Res 2003; 36: 692-700.

[4] Sato O, Hayami S, Einaga Y, Gu Z-Z. Control of the magnetic and optical properties in molecular compounds by electrochemical, photochemical and chemical methods. Bull Chem Soc Jpn 2003; 76: 443-70.

[5] Sato O, Iyoda T, Fujishima A, Hashimoto K. Photoinduced magnetization of a cobalt-iron cyanide. Science 1996; 272: 704-5.

[6] Li G, Akitsu T, Sato O, Einaga Y. Photoinduced magnetization of the Cyano-bridged 3d-4f heterobimetallic assembly $Nd(DMF)_4(H_2O)_3(\mu\text{-}CN)Fe(CN)_5H_2O$ (DMF = N,N-Dimethylformamide). J Am Chem Soc 2003; 125: 12396-7.

[7] Li G, Sato O, Akitsu T, Einaga Y. Visible light-induced magnetization change of the Cyano-Bridged 3d-4f Heterobimetaric. J Solid State Chem 2004; 177: 3835-8.

[8] Coronado E, Gimenez-Saiz C, Martinez-Agudo JM, Nuez A, Romero FM, Stoeckli-Evans H. Design of chiral magnets: cyanide-bridged bimetallic assemblies based on cyclohexane-1,2-diamine. Polyhedron 2003; 22: 2435-40.

[9] Coronado E, Gomez-Garcia CJ, Nuez A, Romero F M, Rusanov E, Stoeckli-Evans H. Ferromagnetism and chirality in two-dimensional Cyanide-Bridged bimetallic compounds. Inorg Chem 2002; 41: 4615-7.

[10] Coronado E, Gimenez-Saiz C, Nuez A, Sanchez V, Romero F M. Stoichiometric control of the magnetic properties in Copper(II) Cyano-Bridged bimetallic complexes. Eur J Inorg Chem 2003; 2003(24): 4289-93.

[11] Kaneko W, Kitagawa S, Ohba M. Chiral Cyanide-Bridged $Mn^{II}Mn^{III}$ Ferrimagnets, $[Mn^{II}(HL)(H_2O)][Mn^{III}(CN)_6]\cdot 2H_2O$ (L = *S*- or *R*-1,2-diaminopropane): Syntheses, structures, and magnetic behaviors. J Am Chem Soc 2007; 129: 248-9.

[12] Imai H, Inoue K, Ghalasaki PS, *et al.* You have full text access to this content Three-Dimensional chiral molecule-based ferrimagnet with triple-helical-strand structure. Angew Chem Int Ed 2004; 43: 5618-21.

[13] Inoue K, Kikuchi K, Ohba M, Okawa H. Structure and magnetic properties of a chiral two-dimensional ferrimagnet with T_C of 38 K. Angew Chem Int Ed 2003; 42: 4810-3.

[14] Geisheimer AR, Karz MJ, Batchelor RJ, Leznoff DB. Preparation and characterization of two chiral $Au(CN)_2$-based coordination polymers containing (1*R*,2*R*)-*N*,*N′*-dimethylcyclohexanediamine. CrystEngComm 2007; 9: 1078-83.

[15] Escax V, Champion G, Arrio M-A, Zacchigna M, Cartir dit Moulin C, Bleuzen A. The Co Ligand Field: A key parameter in photomagnetic cofe prussian blue derivatives. Angew Chem Int Ed 2005 ; 44 : 4798-801.

[16] Cartir dit Moulin C, Champion G, Cafun J-D, Arrio M-A, Bleuzen A. Structural rearrangements induced by photoexcitation in a RbCoFe prussian blue derivative. Angew Chem Int Ed 2007; 46: 1287-9.

[17] Goodwin AL, Chapman KW, Kepert CJ. Guest-dependent negative thermal expansion in nanoporous prussian blue analogues $M^{II}Pt^{IV}(CN)_6\cdot x\{H_2O\}$ $(0 \leq x \leq 2$; M = Zn, Cd). J Am Chem Soc 2005; 127: 17980-1.

[18] Chapman KW, Chupas PJ, Kepert CJ. Compositional dependence of negative thermal expansion in the prussian blue analogues $M^{II}Pt^{IV}(CN)_6$ (M = Mn, Fe, Co, Ni, Cu, Zn, Cd). J Am Chem Soc 2006; 128: 7009-14.

[19] Sereda O, Neels A, Stoeckli F, Stoeckli-Evans H. Chiral bimetallic assemblies and coordination polymers based on tetracyanonickelate: a striking reversible structural transformation. Crystal Growth Des 2008; 8: 3380-4.

[20] Akitsu T, Einaga Y. Extremely long axial cu-n bonds in chiral one-dimensional zigzag cyanide-bridged Cu^{II}-Ni^{II} and Cu^{II}-Pt^{II} bimetallic assemblies. Inorg Chem 2006; 45: 9826-33.

[21] Akitsu T, Einaga Y. Tuning of electronic properties of one-dimensional cyano-bridged Cu^{II}-Ni^{II}, Cu^{II}-Pd^{II}, and Cu^{II}-Pt^{II} bimetallic assemblies by stereochemistry of ligands. Inorg Chim Acta 2008; 361: 36-42.

[22] Akitsu T, Einaga Y. Thermal and photo-responsibility of axial semi-coordination bonds in a Copper(II) complex. Bull Chem Soc Jpn 2004; 77: 763-4.

[23] Akitsu T, Einaga Y. Bis(N-ethyl-ethylenediamine-N,N')copper(II) hexacyanocobalt(III) water (3/2/4): Two-dimensitonal ladder structure of bimetallic assembly. Acta Crystallogr 2006; E62: m750-m2.

[24] Akitsu T, Einaga Y. A redetermination of bis(N-methylethylenediamine-κ^2-N,N’)bis(perchlorate-kO)copper(II). Acta Crystallogr 2003; E59: m991-3.

[25] Akitsu T, Einaga Y. Bis(N,N-dimethylethylenediamine-κ^2-N,N,) bis(perchlorate-kO)copper(II). Acta Crystallogr 2004; E60: m234-6.

[26] Akitsu T, Einaga Y. Bis(acetone-kO)(N,N'-methylethylenediamine-κ^2-N,N,)copper(II)diperchlorate. Acta Crystallogr 2004; C60: m162-4.

[27] Akitsu T, Einaga Y. Structures, magnetic properties, and XPS of one-dimensional cyanide-bridged Cu^{II}–Ni^{II}/Pt^{II} bimetallic assembly complexes. Inorg Chim Acta 2007; 360: 497-505.

[28] Akitsu T, Endo Y. The one-dimensional chain structure of $Cu(N\text{-}Eten)_2Pd(CN)_4$ (N-Eten = N-ethylethylenediamine). Acta Crystallogr 2009; C65: m406-7.

[29] Akitsu T, Einaga Y. The one-dimensional chain structure of $[Cu(en)_2Pt(CN)_4]$ (en is ethylenediamine). Acta Crystallogr 2006; E62: m862-4.

[30] Akitsu T, Einaga Y, Yoza K. Thermally-accessible lattice strain and local pseudo jahn-teller distortion in various dimensional Cu^{II}-M^{III} bimetallic cyanide-bridged assemblies. Open Inorg Chem J 2008; 2: 1-10.

[31] Pariya C, Liao F-L, Wang S-L, Chung S-L. Syntheses, crystal structures and solid state thermochromism of copper(II) complexes of *trans*-1,2-diaminocyclohexane. Polyhedron 1998; 17: 547-54.

[32] Sheldrick GM. A short history of SHELX. Acta Crystallogr 2008; A64: 112-22.

[33] Bruker. *SMART and SAINT*. Bruker AXS Inc., Madison, Wisconsin, USA, 1998.

[34] Sheldrick GM. *SADABS*. Program for empirical absorption correction of area detector data, University of Gottingen, Germany, 1996.

[35] Hathaway BJ, Billing DE. The electronic properties and stereochemistry of mono-nuclear complexes of the copper(II) ion. Coord Chem Rev 1970; 5: 143-207.

[36] Bondi A. van der Waals Volumes and Radii. J Phys Chem 1964; 68: 441-51.

[37] Evans JSO. J. Negative thermal expansion materials. J Chem Soc Dalton Trans 1999: 3317-26.

[38] Falvello LR. Jahn-Teller effects in solid-state co-ordination chemistry. J Chem Soc Dalton Trans 1997: 4463.

[39] Halcrow MA. Interpreting and controlling the structures of six-coordinate copper(II) centres – When is a compression *really* a compression? Dalton Trans 2003: 4375-84. dio:10.1039/β309242A.

[40] Nakamoto K. *Infrared, Raman Spectra of Inorganic and Coordination Compounds*, 3rd ed. Wiley: New York 1978.

[41] Lever ABP. *Inorganic Electronic Spectroscopy*, 2nd ed. Amsterdam: Elesevier: 1984.

[42] Akitsu T, Komorita S, Tamura H. Tuning of electronic properties of one-dimensional cyano-bridged Cu^{II}–Ni^{II}, Cu^{II}–Pd^{II}, and Cu^{II}–Pt^{II} bimetallic assemblies by stereochemistry of ligands. Inorg Chim Acta 2003; 348: 36-42.

[43] Akitsu T, Komorita S, Urushiyama A. Assignment of d–d transitions of square planar $[Cu^{II}N_4]$ complexes containing imidate and amine ligands by means of polarized crystal spectra. Bull Chem Soc Jpn 2001; 74: 851-60.

[44] Zhang H, Cai J, Feng X-L, *et al*.-N. Polyhedron 2002; 21: 721-8.
[45] Kuchar J, Cernak J, Mayerova Z, Kubacek P, Zak Z. Preparation, spectral properties and structures of $Cu(L_N)_xNi(CN)_4$ (L_N = N-methylated Derivates of 1,2-diaminoethane; x = 1,2). Solid State Phenom 2003; 90-91: 323-8.
[46] Cernak J, Chomic J, Gravereau P, *et al*. Chain-like crystal structure and magnetic properties of [catena-bis(1,2- diaminoethane) copper(II)-μ-dicyano-argentate]-dicyanoargentate. Inorg Chim Acta 1988; 281: 134-40.
[47] Cernak J, Skorsepa J, Abboud KA, *et al*. Preparation, crystal structure and magnetic properties of $Cu(en)_2Pd(CN)_4$. Inorg Chim Acta 2001; 326: 3-8.

Received: July 17, 2010 Revised: December 29, 2010 Accepted: January 09, 2011